Canadian Journal of Remote Sensing
Journal canadien de télédétection

Exploring the Influence of Impervious Surface Density and Shape on Urban Heat Islands in the Northeast USA using MODIS and Landsat

Journal:	*Canadian Journal of Remote Sensing*
Manuscript ID:	CJRS-11-0131
Manuscript Type:	Research Article
Date Submitted by the Author:	13-Nov-2011
Complete List of Authors:	Zhang, Ping; NASA GSFC, Code 618 Imhoff, Marc; NASA GSFC, Code 618 Bounoua, Lahouari; NASA GSFC, Code 618 Wolfe, Robert; NASA GSFC, Code 619
Keyword:	urban, temperature, land cover

Exploring the Influence of Impervious Surface Density and Shape on Urban Heat Islands in the Northeast USA using MODIS and Landsat

Ping Zhang[1, 2], Marc L. Imhoff[1], Lahouari Bounoua[1] and Robert E. Wolfe[1]

1. Hydrospheric and Biospheric Science Laboratory, NASA's Goddard Space Flight Center, Greenbelt, MD, 20771, USA
2. Earth Resource Technology Inc., Annapolis Junction, MD, 20701, USA

Send correspondence to:

Ping Zhang

Biospheric Sciences Branch Code 618

NASA's Goddard Space Flight Center

Greenbelt, MD, 20771, USA

Tel.: 301-614-6698

Fax: 301-614-6695

Ping.zhang-1@nasa.gov

Abstract:

Impervious surface area (ISA) from the National Land Cover Database (NLCD) 2001 and land surface temperature (LST) from MODIS averaged over three annual cycles (2003-2005) are used in a spatial analysis to assess the urban heat island (UHI) signature and its relationship to settlement size and shape, development intensity distribution, and land cover composition for 42 urban settlements embedded in forest biomes in the Northeastern United States. Development intensity zones, based on percent ISA, are defined for each urban area emanating outward from the urban core to nearby rural areas and are used to stratify land surface temperature. The stratification is further constrained by biome type and elevation to insure objective intercomparisons between urban zones within an urban settlement and between settlements. Stratification based on ISA allows the definition of hierarchically ordered urban zones that are consistent across urban settlements and scales.

In addition to the surrounding ecological context, we find that the settlement size and shape as well as the development intensity distribution significantly influence the amplitude of summer daytime UHI. Within the Northeastern US temperate broadleaf mixed forest, UHI magnitude is positively related to the logarithm of the urban area size. Our study indicates that for similar urban area sizes, the development intensity distribution is one of the major drivers of UHI. In addition to urban area size and development intensity distribution, this analysis shows that both the shape of the urban area and the land cover composition in the surrounding rural area play an important role in modulating the UHI magnitude in different urban settlements. Our results indicate that remotely sensed urban area size and shape as well as the development intensity distribution influence UHI amplitude across regional scales.

Introduction:

The urban heat island (UHI) is a direct consequence of urban land transformation and is of interest across science disciplines because it affects human health and activities, ecosystem function, energy use, local weather and possibly climate. The UHI phenomenon has several causes but is generally seen as being caused by a reduction in latent heating at the expense of sensible heating in urban areas where vegetated and evaporating soil surfaces have been replaced by heat absorbing impervious paving and building materials, thereby creating a difference in temperature between urban and surrounding non-urban areas (Oke, 1982; Owen et al. 1998; Yuan and Bauer, 2006).

Previous studies have found that the UHI intensity is related to many factors including albedo (e.g. Taha 1997; Rosenzweig et al. 2010), wind speed (e.g. Unger et al. 2001), cloud cover (e.g. Morris et al. 2001), urban geometry (e.g. Oke et al. 1991; Arnfield, 1990), and thermal properties (e.g. Oke et al. 1991). It is worth noting however that most of these studies have focused on one specific urban area and may then be considered as localized case-studies. The intercomparison of UHI effect across cities and scales has been hampered by the lack of objectively quantifiable indicators, commonly agreed upon definitions for urban density and urban versus non-urban areas. Although population count is not a physical quantity, because of its availability for long periods of time and over different cities, it is frequently chosen to represent the city's level of urbanization (e.g. Oke, 1973, 1976; Karl et al. 1988; Camillioni and Barros, 1997). Previous studies have found that the UHI intensity is strongly and positively related to the logarithm of the population of cities in North America and Europe (Oke, 1973, 1976; Lansberg, 1981), even though population data is usually collected within somewhat arbitrary boundaries and is not a direct indicator of UHI.

More recent studies (e.g. Imhoff et al. 2010 and Zhang et al. 2010) used remotely-sensed impervious surface area (ISA) as an indicator of the extent and intensity of urbanization for UHI analysis regionally and globally. The size of an urban settlement was estimated as the total contiguous area of each urban polygon with more than a 25% ISA threshold. As an indicator of urbanization, ISA appears more objective than population and can be consistently applied across large scale areas allowing inter-comparisons between distant urban settlements. Imhoff et al. (2010) found that the amplitude of the UHI depends on the surrounding ecological context. They argue that the degree to which urbanization alters the landscape is relative to what was there before the change took place and suggest that the ecological context significantly modulates the amplitude of the UHI. They also point out that UHI is a relative measure where the biophysiology of both the urban core and surrounding non-urban areas are at play. Indeed, in the continental U.S, that study showed that the largest observed UHIs occurred in cities built in forested areas whereas cities located in desert environments pointed to weak UHIs and sometimes even to an urban heat sink (Imhoff et al. 2010). These observations-based results are in line with previous modeling studies of the impact of urbanization on local surface climate (Shepherd 2006; Bounoua et al. 2009).

Zhang et al. (2010) examined the effects of latitudinal stratification on the amplitude of the summer surface UHI at a global scale and showed that mid-latitude urban settlements tend to generate larger UHIs than those in tropical and high-latitude areas. They also confirmed that at global scale, UHI amplitude is positively correlated to the size of urban settlements with a consistent pattern of an average summer daytime surface temperature UHI of 4.7 ^{o}C for settlements larger than 500 km^2 compared to only 2.5 ^{o}C for those settlements smaller than 50 km^2 (Zhang et al. 2010).

While previous research focused on the effects of surrounding ecological context on UHI, this study uses a combination of remotely-sensed indicators to explore additional potential drivers of the UHI at a regional scale in the Northeastern U.S.

Data and Methodology

2.1. Classification of Urban Density

We use the ISA data from the continental scale National Land Cover Dataset (NLCD, Yang et al., 2002). The fractional ISA data were derived using Landsat 7 ETM+ and IKONOS at nominal 30 m spatial resolution discriminating man-made surfaces from natural or vegetated lands (Yang et al., 2002). While the ISA does not contain retrievable information about albedo or 3-D structure, it captures the urban development intensity as a function of the extent and spatial distribution of collections of man-made surfaces within a pixel. Based on ISA, the intensity of the land cover conversion can be related to changes in land surface physical properties including its ability to convert incoming solar energy into sensible and latent heat fluxes at the land-atmosphere interface (e.g. Bounoua et al. 2009). Recently, Yuan and Bauer (2007) and Xian and Crane (2005) demonstrated that the NLCD ISA can be used to make rigorous comparisons of urban density and surface temperature at local scales provided appropriate temperature data are available.

Using a Geographic Information System-based spatial analysis, we identify individual urban areas, stratify them internally according to their ISA fractions, and estimate their sizes. We use the 25% ISA contour as a minimum threshold to define urban polygons in the Landsat-based thematic data. The 25% threshold provides a boundary between urban and low intensity residential lands (Lu and Weng 2006) that is useful for urban studies and has been shown to

delineate spatially coherent urban groupings for cities across broad regions (Imhoff et al., 2010). This method produces a repeatable land cover-based metric of urban areas which do not necessarily match legally incorporated or cadastral (administrative) boundaries.

Once urban clusters are defined, we further stratify the landscape within and around them using classes based on ISA fractions and distance. For an extensive spatial analysis, we define five zones based on classes of percent ISA in concentric rings emanating outward from the highest ISA in a city to the lowest: 1) Urban Core: composed of pixels having 75 to 100% ISA (these are the highest ISA in a city polygon); 2) Urban1: including pixels having ISA between 75% and 50% ($75\% > ISA \geq 50\%$); 3) Urban2: containing pixels having between 50 and 25% ISA ($50\% > ISA \geq 25\%$) – this is the last urban zone and its outer boundary coincides with the 25% ISA threshold; 4) Suburban: composed of pixels having less than 25% ISA located in a buffer zone of 0-5 km width, adjacent to and outside the 25% ISA contour; and finally 5) Rural (or non-urban) zone composed of pixels located in a 5 km wide ring located between 15 and 20 km away from the 25% ISA contour (Figure 1). The rural zone is chosen to be at an optimal distance far enough from the urban core to represent a relatively remote rural area yet not too far to infringe into the 25% contour of an adjacent urban area or another land cover biome. In the following sections, the urban area is defined as the whole area including Urban Core, Urban1, and Urban2 and the urban heat island (UHI) is obtained as a land surface temperature (LST) difference between Urban Core (or Urban1 when Urban Core is not available, or Urban2 when Urban Core and Urban1 are not available) and the rural zone.

2.2. Land Surface Temperature (LST)

To characterize the surface temperature within the different zones, we use MODIS-Aqua Version 5, 8-day composite (MYD11A2) LST with highest quality control (Wan et al., 2004) at 1 km x 1 km spatial resolution averaged over the period 2003 to 2005. The Aqua LST products are available from 2003 and the 3 year-average is chosen to reduce the natural interannual variation in the temperature field. LSTs from MYD11A2 are retrieved from clear-sky (99% confidence level) observations at 1:30 PM and 1:30AM using a generalized split-window algorithm (Wan and Dozier 1996). Comparisons between MODIS LST's and in-situ temperature measurements across a large set of test sites indicate an LST accuracy better than 1^{o} K with an RMS (of differences) less than 0.5^{o} K in most cases (Wan 2008, Wang et al. 2008). The LST data are used to characterize the horizontal temperature gradient across the different zones of the urban area. In this study, temperature data collected for an individual urban area are included in the analysis only if they remain within its dominant vegetation biome type. This eliminates cross-over into different bio-climatic environments as a potential contaminant of the observed temperature differences within an urban area and allows grouping and comparison of UHI effects by biome type. Furthermore the urban and rural temperatures are obtained over their respective zones. This way the difference between the urban and rural temperature (UHI) is representative of the entire urban area and its surrounding rural area, a notable difference from previous work using only few stations to represent the whole region (e.g. Jauregui et al. 1992; Morris and Simmonds 2001). The extensive spatial coverage and the powerful selective methodology used in the present work reduces the bias due to the distribution of ground stations' temperature found in previous studies, strengthens the statistical robustness of the urban-rural temperature differences and provides an objective means for intercomparison between different settlements of different regions.

2.3. Topography and Terrestrial Ecoregion Map

Topographic data are used as a filter to exclude from the analysis temperature differences due to elevation and shading. We use the 30 arc-second (~925 m) spatial resolution SRTM30 (Farr and Kobrick, 2000) dataset to determine a mean elevation of the urban area and exclude from analysis all pixels whose elevation is outside the +/- 50 meters interval from the mean elevation.

To allow comparisons of urban zones within and between urban areas, we use the terrestrial ecoregions map (Olson et al., 2001) to stratify the analysis and constrain the sampling around each urban area according to its biome type. The ecoregions map divides the continental United States into 10 biomes each representing an assemblage of biophysical, climate, botanical and animal habitat characteristics defining a distinct geographical area. Cities from the same biome may have different local climate, biophysical or environmental characteristics.

In addition to the terrestrial ecoregion map, the tree canopy density (Huang et al. 2001, and Homer et al. 2004) derived from the NLCD at 30 m resolution and land cover maps from MODIS at 1 km resolution (Friedl et al. 2002) are used in this research to assess the rural area land cover components on the UHI magnitude.

Results and Discussion

Within the terrestrial ecoregion map, we identified 42 Landsat-ISA-based urban areas in the Northeast US distributed across the broadleaf mixed-forest biome (Figure 1). Since the UHI is a relative measure representing the temperature difference between urban and rural areas, the

ecological context is a strong determinant of its amplitude and large UHIs are found in urban areas surrounded by this biome (Imhoff et al. 2010). For each urban area, a spatial stratification defining the five zones is applied. To characterize the UHI, we calculated the difference between the average temperature of the Urban Core (or Urban1 when Urban Core is not available, or Urban2 when Urban Core and Urban1 are not available) and the Rural area for all cities during summer (June/July/August) and winter (December/January/February) daytime (1:30 PM) and nighttime (1:30 AM) when surface temperatures are near their extremes (Roth et al. 1989, Imhoff et al. 2010, Zhang et al. 2010). Pixels containing a significant fraction of water such as rivers, lakes, reservoirs, and ocean shoreline were eliminated from the analysis in order to reduce the influence of water bodies on the surface temperature data .

3.1 UHI and urban area size

In this analysis, the size of an urban area is defined as the total contiguous area of all urban polygons having an ISA higher than the 25% threshold (Figure 1). Our analysis indicates that the summer daytime UHI is strongly correlated to the urban area size (R^2 = 72%). Indeed, among the 42 sampled urban areas, the averaged UHI is about 1.5^{o} C for urban areas with sizes smaller than 10 km^2, 8 ^{o}C for cities with sizes around 100 km^2 and about 10 ^{o}C for urban areas larger than 1000 km^2 (Figure 2A). This relationship holds true during the winter but with much weaker UHI amplitudes ranging from about 1.0 ^{o}C for urban areas smaller than 10 km^2 to 3.5 ^{o}C for urban areas larger than 1000 km^2. A similar result is observed during the nighttime. Note that unless otherwise specified, when use the term UHI below, we are referring to the summer daytime UHI.

Within the Northeastern temperate forest, the relationship between the UHI amplitude and the urban area size is consistent among all cities (Figure 2A). The relationship is log-linear and explains about 72 % of the variance in UHI with a standard error of ±1.6^{o} C. This result is similar to the log-linear relationship between the UHI and the population size described in Oke (1973 and 1976) and Landsberg (1981).

An important conclusion emanating from this work is that the logarithmic relationship between UHI amplitude and urban size as delineated using the ISA data is confirmed in the 42 sampled Northeastern US urban areas using relatively coarse spatial resolution satellite data. This suggests that well calibrated 1km MODIS LSTs data collected over long temporal baselines are capable of resolving the temperature differences between urban and surrounding rural areas in different settlements determined by higher spatial resolution satellite data sets like the 30 m Landsat ISA. Furthermore, the spatial stratification used in this study and its precursor (Imhoff et al. 2010) is adequate to capture UHI signals similar to those obtained using carefully selected air temperature stations within urban and rural areas (Oke, 1973).

3.2 UHI and urban shape

We also examine the relationship between UHI magnitude and the degree of aggregation of the corresponding urban area. Quantifying the aggregation level and the degree of clumpiness of spatial patterns is often useful in relating patterns to ecological processes (Sisk et al., 1997). Many quantitative indices have been used to characterize landscape patterns and to examine relationships between them and ecological processes, such as the contagion index (O'Neill et al. 1988; Riitters et al. 1996), the patch cohesion index (Schumaker 1996), and the aggregation index (He et al, 2000). In this analysis, we use the area to perimeter (A/P) ratio to characterize

the degree of clumpiness and cohesion of each urban area. In general for urban areas of similar size, the larger the area to perimeter ratio (A/P), the more clumpy and aggregated the urban area is and a more significant UHI effect would be expected.

Using the 42 sampled cities, we found that the A/P ratio explains 70% of the variance in UHI with a logarithmic relationship similar to that of the urban area size and population count (Figure 2B). However, even though the relationships between UHI and urban area size and A/P ratio are similar, the effects of these two landscape indicators are quite different for individual cities. For example, for cities with similar urban area size: Syracuse NY (152 km^2) vs. Harrisburg PA (153 km^2), our results indicate that the UHI is more intense at Syracuse (10.6 ^oC) than at Harrisburg (7.6 ^oC) (Table 1). These two cities appear as outliers in Figure 2A where, taken separately, the urban area cannot account for the total UHI difference. Interestingly, the A/P ratio appears to be a better indicator of the UHI amplitude for these two cities with same area sizes but quite different shapes (Figure 2B).

Figure 3A shows the histogram of the impervious pixels inside the urban area boundaries of Syracuse and Harrisburg. The two urban areas have similar ISA histogram distributions. From a calculated percentage (not shown), it appears that about one third of the urban pixels has 25-50% of ISA, one fourth has 50-75% of impervious surface area, and one fifth of the urban pixels has more than 75% ISA. However, the geometry of the urban area around the two cities is quite different. This is indicated by the A/P ratio (table 1) and clearly visible from the ISA spatial distribution (Figure 4A) which shows the impervious surface area for Syracuse more clumpy and centralized than for Harrisburg, resulting in a stronger urban core warming and a more intense UHI than Harrisburg.

For an intercomparison between urban areas, we normalize the A/P ratio to remove its dependence on the area size. We compute a normalized A/P ratio as the A/P ratio of the actual urban area divided by the A/P ratio of a hypothetical circular urban area with the same size. This way, the larger the normalized A/P ratio, the more centralized "Clumpy" the city will be while decentralized "fragmented" urban areas will be associated with small normalized A/P ratios. For all 42 urban areas selected in this study, figure 5 shows that as the urban area grows the normalized A/P ratio decreases, suggesting a general pattern of fragmentation. In general, small urban areas tend to be more centralized than larger ones. Our study shows that for urban areas with similar sizes, the fragmented ones have a smaller UHI magnitude than those with centralized shapes.

3.3 UHI and land cover component

In previous sections, our analysis clearly shows the size, shape and ISA density are important drivers of the UHI difference in most Northeastern US urban areas. The comparative case study of Syracuse and Harrisburg shows that while the urban area size cannot entirely explain the UHI difference between these two cities, the shape of the urban area, characterized by its area to perimeter ratio, explains a significant part of the difference. However, there remain outlier urban areas with approximately the same size and A/P ratio and for which the UHI is not fully explained by these indicators. This suggests that other factors may play a role in defining the urban-rural temperature difference. Examples of such outlier urban areas are Providence RI and Buffalo NY with an UHI of 12.2 ^{o}C and 7.2 ^{o}C, respectively. Such important difference in UHIs generated in the two urban areas cannot be explained either by the size of urban area (Fig. 2A) or by the area/perimeter ratio (Fig. 2B). Our results show that Providence has a warmer

temperature in its urban core and a cooler temperature in the surrounding rural area compared to Buffalo (Table 1).

We explored additional drivers including the ISA distribution inside the urban area and the land cover composition in the rural area. Figure 3B shows the ISA histogram inside the urban boundary around these two cities. Even though the two cities have about the same urban area size, their ISA distributions are quite different. Specifically, more than 33% of the urban pixels in Providence are within the Urban Core (75 < ISA < 100%) while more than 35% are within Urban1 (50 < ISA < 75%) and about 17% are within Urban2 (25 < ISA < 50%). In contrast, the corresponding fractions in Buffalo, for the Urban Core, Urban1 and Urban2 zones are 23%, 23% and 34%, respectively. Therefore, even with similar size as Buffalo, Providence's urban structure is skewed towards higher density ISA and generates a much warmer urban surface temperature, which is clearly shown from ISA spatial distribution in Figure 4B.

Following Olson et al (2001) both Providence and Buffalo are located in forested biomes, however, using a more detailed MODIS land cover map (Friedl et al. 2002), we find that about 72% of the rural pixels surrounding Providence are classified as forest whereas more than 90% of the rural area of Buffalo is labeled cropland. This is consistent with the tree canopy density (Huang et al. 2001, and Homer et al. 2004) derived from the NLCD at 30 m resolution which shows Providence rural area to have an average tree cover fraction of 84% compared to only 15% for Buffalo (Table 1). In general, trees tend to maintain lower temperature around them as dense foliage reduces the amount of heat reaching the soil and urban structures, and to cool the air through transpiration. Consequently, the surrounding rural area in Providence is about 3 ^{o}C cooler than that in Buffalo, clearly indicating that the high UHI observed in Providence is due to

both a high urban core temperature caused by the high density ISA and a low rural temperature maintained by denser rural vegetation.

The analysis of these two cities serves as a reminder that the UHI is a relative measure and its magnitude is not controlled by the composition of urban area alone, but by the surrounding rural land cover as well, in agreement with the results from Imhoff et al. (2010) and Zhang et al. (2010).

To further explore how the ISA density affects the UHI amplitude, we choose the remaining six urban areas ranging from 100 to 200 km^2 around the cities of: Scranton PA, Worcester MA, Springfield MA, Roanoke VA, Rochester NY, and Albany NY. These six urban areas have different shape characteristics (Figure 6) and ISA distribution (Figure 7). In term of ISA distribution, these urban areas can be grouped in three categories: skew-to-high density (Scranton and Worcester), skew-to-low density (Rochester Roanoke), and symmetrically distributed (Albany and Springfield). To quantify the relationship between UHI and density distribution for these sample urban areas, we calculated a skew metric (high/low ratio) using the ratio of the number of urban pixels with ISA values between 60% and 85% to those with ISA between 25% and 50%. Skew-to-high density urban areas will have large high/low ratio (larger than one); skew-to-low density will have small high/low ratio (smaller than one); and symmetrically distributed urban areas will have high/low ratio around one. Our results show that for similar urban area size, the skew-to-high density category tends to generate more intense UHI than the others (Table 2).

4. Concluding Remarks

We combine remote sensing data from two satellite platforms to assess the amplitude and potential drivers of the UHI around 42 Northeastern US cities embedded in forested areas. We use the Landsat ETM+ based NLCD ISA at 30m to examine the horizontal structure of urban areas, stratify them as function of ISA density and calculate the UHI using 1km LST data acquired from the MODIS instrument onboard the Aqua satellite.

Our results show that within the same ecological context, the UHI amplitude is modulated by the size of the urban area, the shape of the urban area, the distribution of ISA inside the urban area, and the land cover composition of the surrounding rural area. We find that a log-linear relationship explaining more than 70% of the variance in UHI exists with either the size of the urban area defined by an ISA fraction larger than 25%, or the shape of the urban area. These results are in agreement with previous studies (e.g. Oke 1973); however the use of ISA as an indicator of the extent and intensity of urbanization appears more objective than population-based methods used in previous studies and can be consistently applied for inter-comparison of UHIs across different urban areas and from different regions. Even though the urban extension we define here does not necessarily match administrative boundaries, this remotely-sensed methodology provides a more accurate description of the geographically-related relationships between land surface temperature, urban area size and shape due to consistent geographic limits within which all variables are obtained.

Exploring additional indicators to explain the variance of the UHI amplitude proved to be successful in some but not all urban areas. In fact, with similar urban area size and total ISA, Syracuse generates a UHI 3 ^{o}C more intense than Harrisburg. This large difference in UHI appears related to the clumpiness and centralization of the spatial distribution of ISA, defined by the area to perimeter ratio. On the other hand, the land cover composition of the surrounding

rural area also modulates the UHI amplitude, as illustrated by the example of Buffalo and Providence. A High urban core ISA and a large tree cover fraction in the surrounding rural area in Providence create a marked temperature contrast as compared to Buffalo.

Combining indicators in multiple linear regression models did not significantly improve the explained variance due most likely to the complexity of the UHI and its non-linear dependence on the urban versus rural energy balance differences (e.g.; Oke 1973, Bounoua et al. 2009). The indicators we use also do not take 3D structural factors into account which are known to influence thermal admittance properties in urban areas (Oleson et al. 2010).

However, within the capabilities of the data used here, our analysis suggests that remotely-sensed ISA and LST provide powerful indicators to characterize the urban area and stratify it as a function of size, ISA density and shape, and to analyze both the magnitude and spatial extent of the UHI with an objective methodology inter-comparable across large-scale regions.

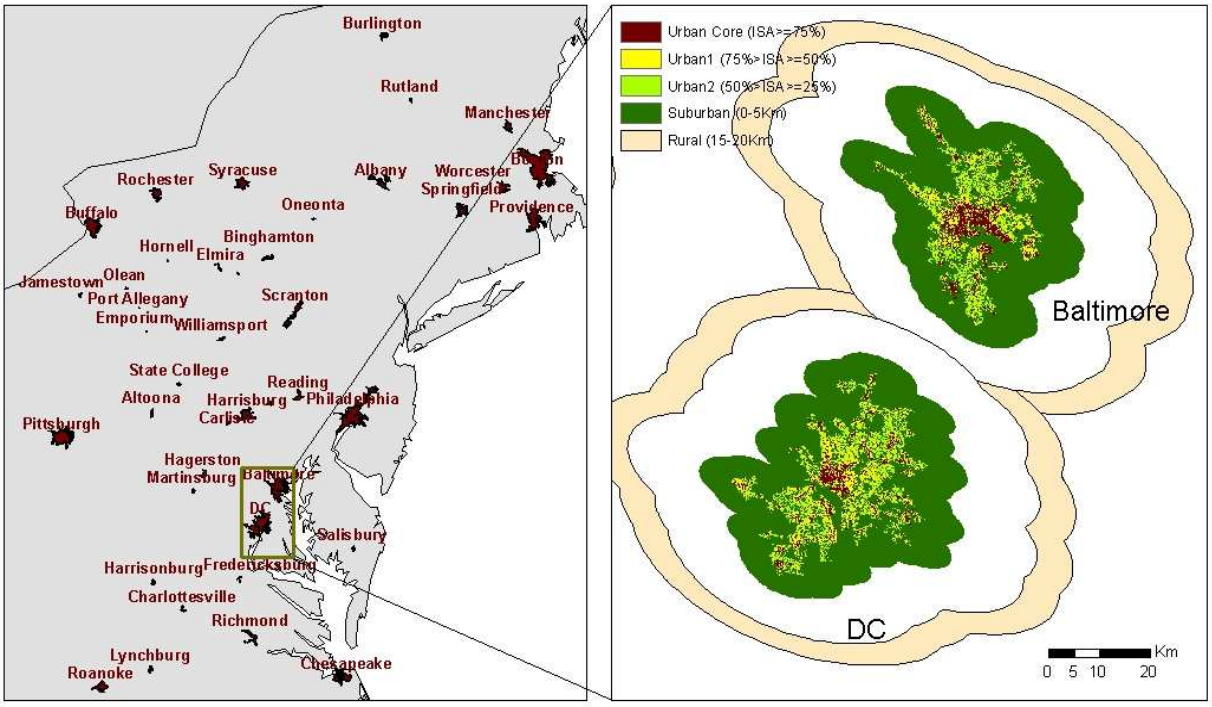

Figure 1: Left panel shows 42 sampled cities in Northeast USA ranging from less than 10 km^2 to more than 1000 km^2 in size. All cities are defined by 25% NLCD ISA contour and are embedded in forest based on the Olson et al. (2001) terrestrial biomes map. Right panel shows an example of typical layout of the 5 zones defined for each city. Urban Core, Urban1 and Urban2 are based on %ISA of each pixel (see text for details). The Suburban zone is composed of pixels with less than 25% ISA occurring within a 5km wide ring adjacent to the 25% ISA contour. The Rural zone is a ring confined between 15 and 20 km distance from the 25% ISA contour and composed of pixels with less than 1% ISA. Pixels that cross biomes or exceed the mean elevation by ± 50m are excluded. UHI (urban - rural) calculations use MODIS temperature (LST) difference between the urban and rural zone (see text for detail).

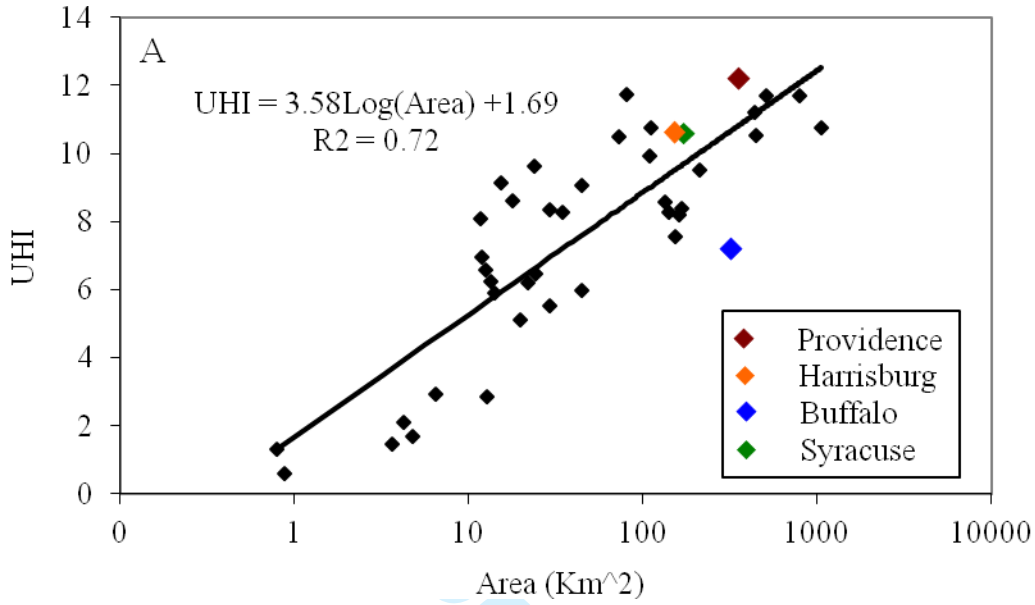

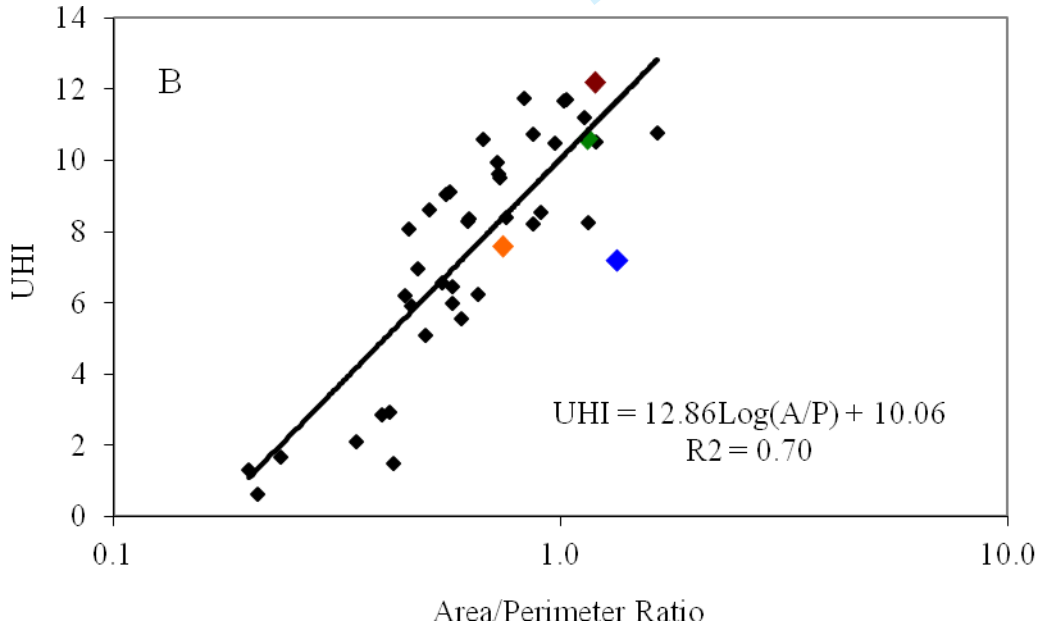

Figure 2: The relationship between the summer daytime UHI (^{o}C) and (A) urban area size (km^2), (B) Area/Perimeter ratio (km) in Northeastern US cities. Four cities are highlighted in colored font as case studies Providence vs Buffalo, Syracuse vs Harrisburg (see text for details).

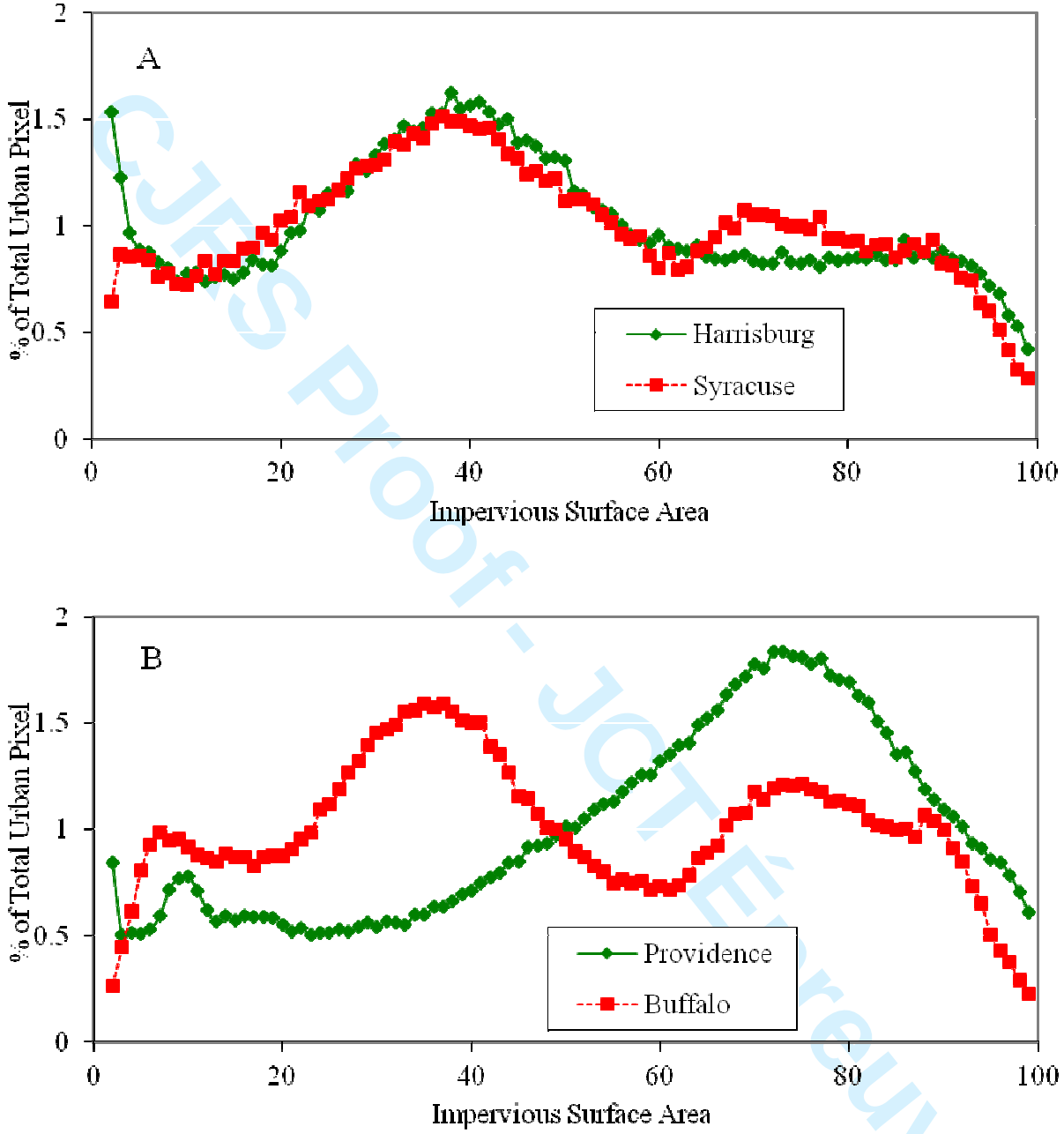

Figure 3: The ISA histogram in Syracuse and Harrisburg (Panel A), Providence and Buffalo (Panel B). X-axis shows the ISA (%) and Y-axis shows the pixel counts as a percentage of the total pixel counts within the urban boundary (25% ISA contour).

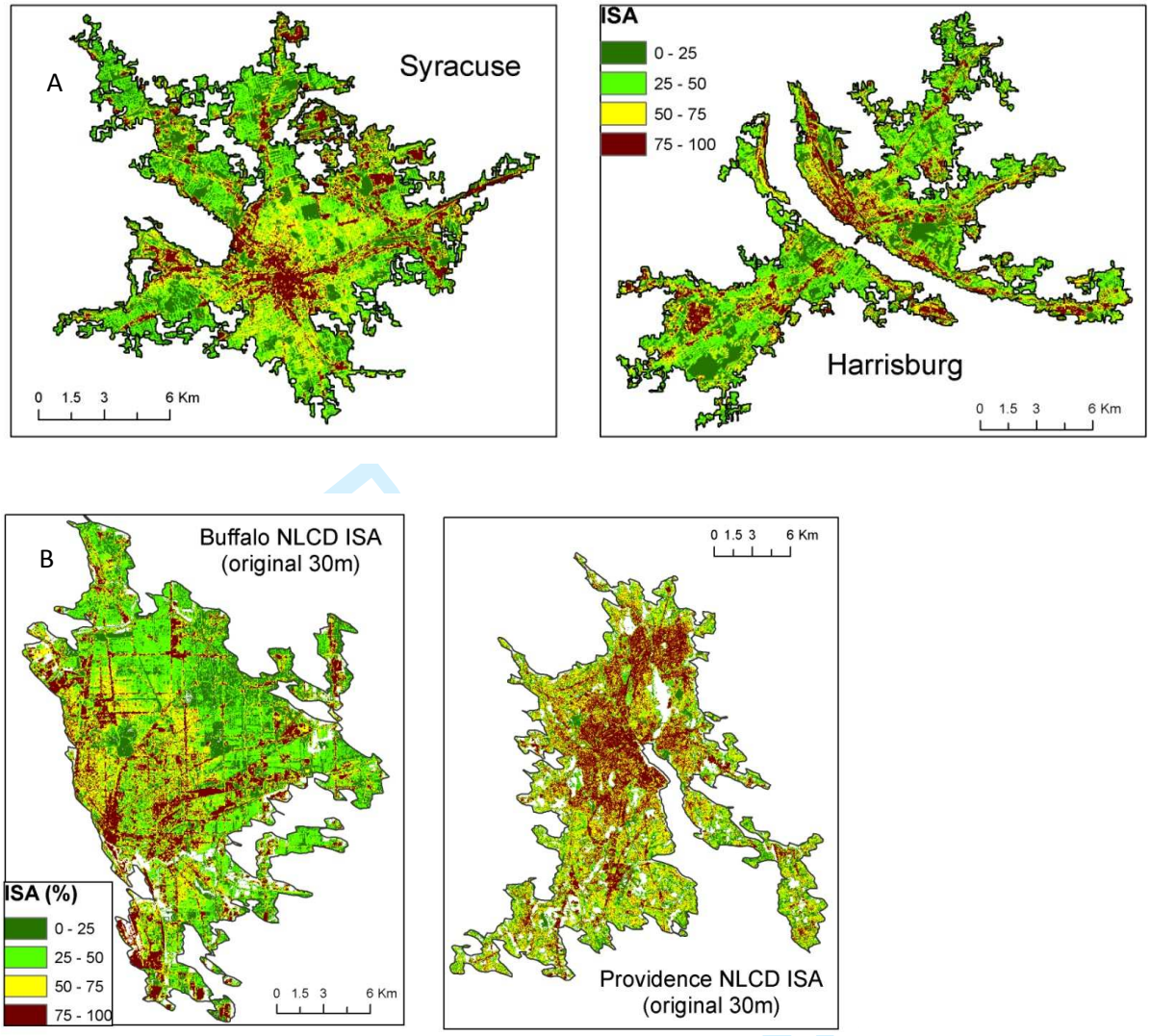

Figure 4: NLCD 2001 Impervious Surface Area in Syracuse and Harrisburg (A), Buffalo and Providence (B) at 30m resolution. The 25% ISA contour is used to define the urban boundary.

Table 1: Urban characteristics for select cities.

	Urban Area (km^2)	Urban A/P (km)	Core Area (km^2)	Tree (%)	Core Temp (° C)	Rural Temp (° C)	UHI (° C)
Providence	356	1.19	98	84	37.2	25.1	12.2
Buffalo	321	1.34	67	15	35.4	28.2	7.2
Syracuse	152	1.15	27	22	36.7	26.0	10.6
Harrisburg	153	0.74	27	32	34.9	27.3	7.6

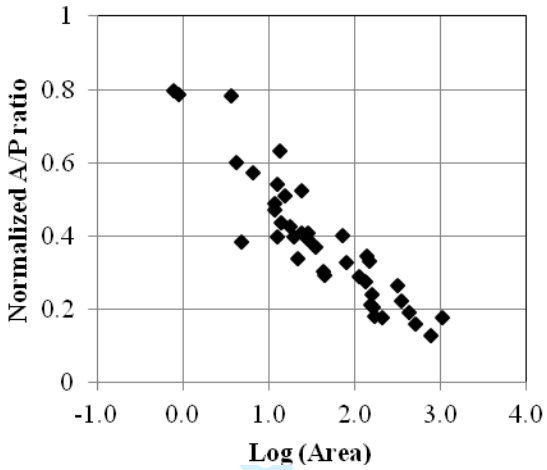

Figure 5: The relationship between urban area and normalized A/P ratio. The normalized A/P ratio is the actual A/P ratio of the urban area divided by the A/P ratio of a hypothetical circular urban area having the same size (see text for detail).

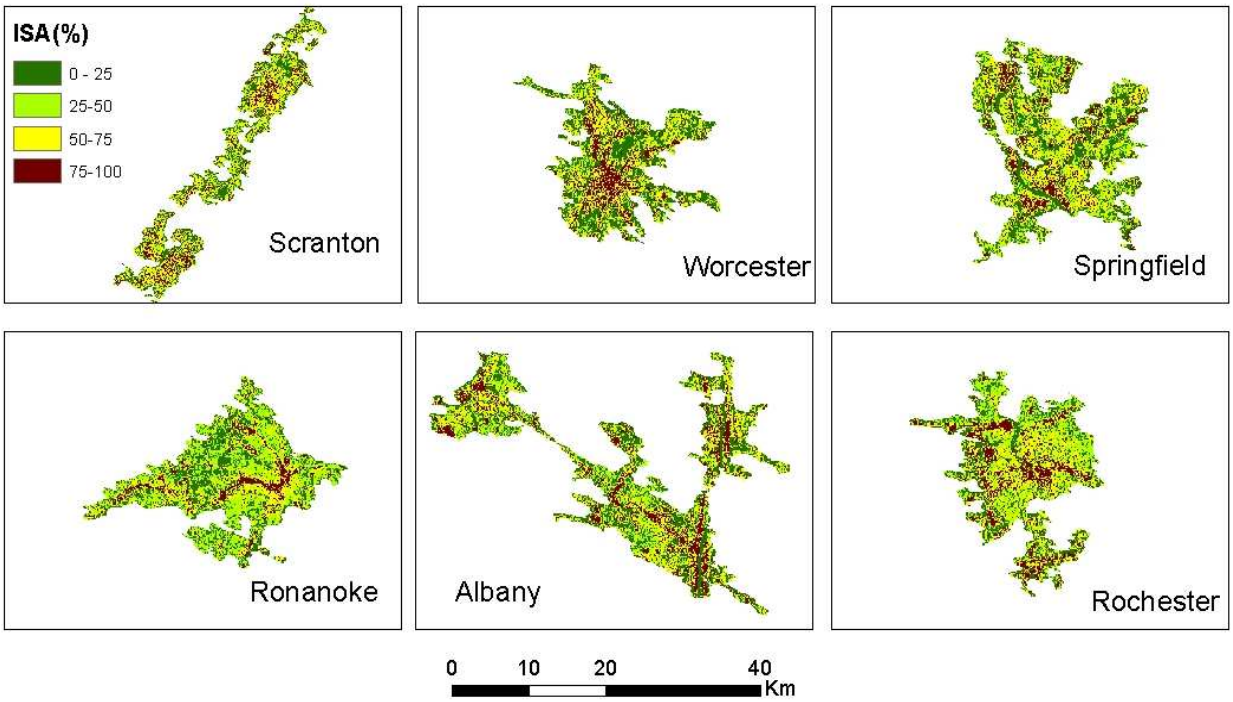

Figure 6: The spatial distribution of impervious surface area for six Northeastern cities with areas ranging from 100 km^2 to 200 km^2. Each urban area is defined by the 25% ISA contour.

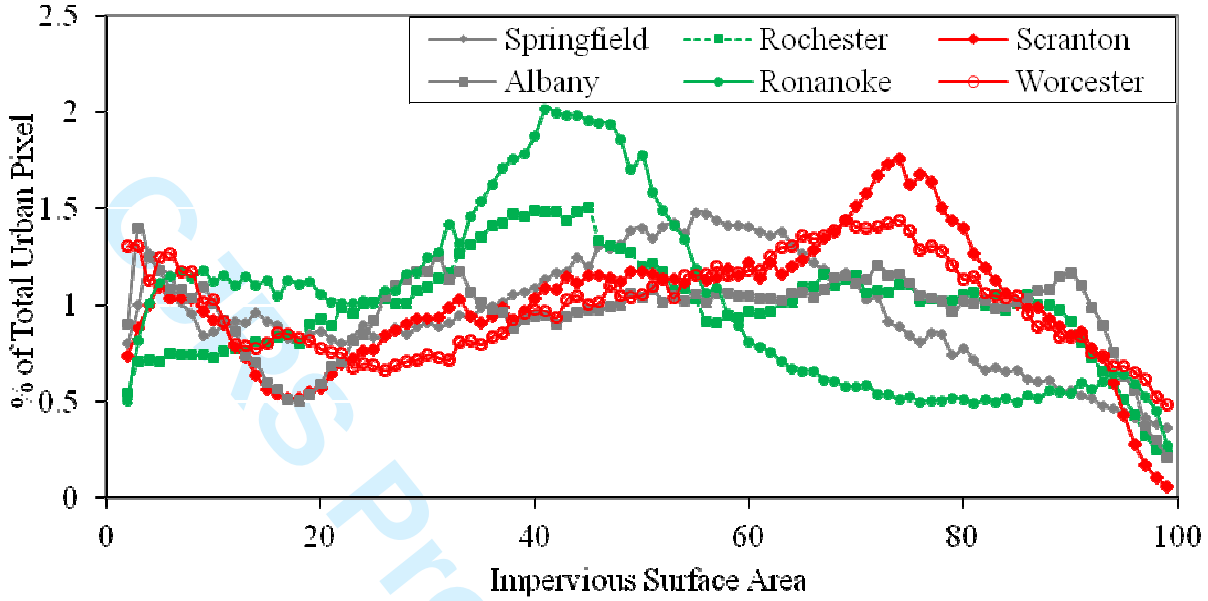

Figure 7: The ISA histogram for six Northeast forest cities with area from 100 km^2 to 200 km^2. X-axis shows the ISA and Y-axis shows the pixel counts as a percentage of the total pixel counts within the urban boundary.

Table 2: Urban characteristics of six Northeast cities with area from 100 to 200 km^2.

City	Class	Skew Metric	Area (km^2)	Tree (%)	UHI (° C)	Rural T (° C)	Core T (° C)
Roanoke	Low-density	0.37	141	63	8.3	27.7	35.9
Rochester	Low-density	0.81	134	7	8.6	26.5	35.0
Worcester	High-density	1.47	112	89	10.7	24.4	35.1
Scranton	High-density	1.39	171	85	10.6	25.5	36.1
Springfield	Symmetrical	0.97	161	89	9.1	26.5	34.7
Albany	Symmetrical	1.04	167	61	8.4	26.1	34.5

Reference:

Arnfield AJ. 1990. Canyon geometry, the urban fabric and nocturnal cooling: a simulation approach. Physical Geography 11: 220–239.

Bounoua, L., A. Safia, J. Masek, C. Peters-Lidard, and M. Imhoff, 2009. Impact of Urban Growth on Surface Climate: A Case Study in Oran, Algeria J. Applied Meteorology Climatology, 48(2), 217-231.

Farr, T.G., and Kobrick, M. 2000. Shuttle Radar Topography Mission produces a wealth of data, Amer. Geophys. Union Eos, Vol. 81, pp. 583-585.

Friedl, M., D.K. McIver, J.C.F. Hodges, X.Y. Zhang, D. Muchoney, A.H. Strahler, C.E. Woodcock, S. Gopal, A. Schneider, A. Cooper, A. Baccini, F. Gao and C. Schaaf , 2002. Global land cover mapping from MODIS: algorithms and early results Special issue . Remote Sensing of Environment 83, pp. 287–302.

He, S.H., B. E. DeZonia and D.J. Mladenoff, 2000. An aggregation index to quantify spatial patterns of landscapes. Landscape Ecology 15, 591-601.

Homer, C. C. Huang, L. Yang, B. Wylie and M. Coan. 2004. Development of a 2001 National Landcover Database for the United States. Photogrammetric Engineering and Remote Sensing, Vol. 70, No. 7, July 2004, pp. 829-840.

Huang, C., L. Yang, B. Wylie and C. Homer, "A Strategy for Estimating Tree Canopy Density Using Landsat & ETM+ and High Resolution Images over Large Areas", The proceedings of the Third International Conference on Geospatial Information in Agriculture and Forestry held in Denver, Colorado, 5-7 November, 2001, 1 disk.

Imhoff, M.L., Zhang, P., Wolfe, R.E., and Bounoua, L. 2010. Remote sensing of urban heat island effect across biomes in the continental USA. Remote Sensing of Environment, Vol. 114, pp. 504-513.

Jauregui, E, Godinez L, Cruz F. (1992), Aspects of heat island development in Guadalajara, Mexico, Atmospheric Environment, 26B(3), 391-396.

Karl, T.R., Diza, H.F., & Kukla, G. (1988). Urbanization: its detection and effect in the United States climate record. *Journal of Climate, 1,* 1099-1123.

Landsberg, E. H. (1981). The Urban Climate. In *International Geophysics Series,* Vol. 28. Page 5. New York: Academic Press.

Lu, D., & Weng, Q. (2006). Use of impervious surface in urban land-use classification. *Remote Sensing of Environment, 102,* 146-160.

Morris CJG, Simmonds I, Plummer N. 2001. Quantification of the influences of wind and cloud on the nocturnal urban heat island of a large city. Journal of Applied Meteorology 40: 169–182.

Oke, T.R. (1973). City size and the urban heat island. *Atmospheric Environment Pergamon Press. 7,* 769-779.

Oke, T.R. (1976). The distinction between canopy and boundary layer urban heat islands. *Atmosphere, 14,* 268-277.

Oke, T.R. 1982. The energetic basis of the urban heat island, *Quarterly Journal of the Royal Meteorological Society* **108**, pp. 1–24.

Oke TR, Johnson GT, Steyn DG, Watson ID. 1991. Simulation of surface urban heat islands under 'ideal' conditions at night. Part 2: diagnosis of causation. Boundary-Layer Meteorology 56: 339–358.

Olson, D.M., Dinerstein, E., Wikramanayake, E.D., Burgess, N.D., Powell, G.V.N., Underwood, E.C., D'Amico, J.A., Itoua, I., Strand, H.E., Morrison, J.C., Loucks, C.J., Allnutt, T.F., Thomas F., Ricketts, T.H., Kura, Y., Lamoreux, J.F., Wettengel, W.W., Hedao, P., & Kassem, K.R. (2001). Terrestrial Ecoregions of the World: A New Map of Life on Earth. *BioScience, 51(11),* 933-938.

O'Neill, R.V., J.R. Krummel, R.H. Gardner, et al. 1998. Indices of landscape pattern. Landscape Ecology 1, 153-162.

Owen, T.W., Carlson, T.N., & Gillies, R.R. (1998). An assessment of satellite remotely-sensed land cover parameters in quantitatively describing the climatic effect of urbanization. *International Journal of Remote Sensing, 19(9),* 1663-1681.

Riitters, K.H., O'Neill, R.H., Wickham, J.D., and Jones, K.B. 1996. A note on contagion indices for landscape analysis. Landscape Ecology 11, 197-202.

Rosenzweig, C., W. D. Solecki, L. Parshall, et al. 2010. Mitigating New York City's Heat Island: Integrating stakeholder perspectives and scientific evaluation. Bulletin of the American Meteorological Society, 1297-1312.

Roth, M., Oke, T.R., and Emery, W.J. 1989. Satellite-derived urban heat islands from three coastal cities and the utilization of such data in urban climatology. Int. J. Remote Sensing, Vol. 10, pp. 1699-1720.

Schumaker, N.H. 1996. Using landscape indices to predict habitat connectivity. Ecology 77, 1210-1225.

Shepherd, J.M., 2006. Evidence of Urban-Induced Precipitation Variability in Arid Climate Regimes, Journal of Arid Environments, 67, 607-628.

Sisk, T.D., N. Haddad, and P.R. Ehrlich. 1997. Bird assemblages in patchy woodlands: modeling the effects of edge and matrix habitats. Ecological Applications 7:1170-1180.

Taha, H., 1997: Urban climates and heat islands: Albedo, evapotranspiration and anthropogenic heat. Energy Build., 25, 99–103.

Unger J, S¨umeghy Z, Zoboki J. 2001. Temperature cross-section features in an urban area. Atmospheric Research 58: 117–127.

Wan, Z., & Dozier, J. (1996). A generalized split-window algorithm for retrieving land-surface temperature from space. *IEEE Transactions on Geoscience & Remote Sensing, 34(4),* 892-905.

Wan, Z., Zhang, Y., Zhang, Q., & Li. Z-L. (2004). Quality assessment and validation of the MODIS land surface temperature. *International Journal of Remote Sensing*, 25, 261-274.

Wan, Z. (2008). New refinements and validation of the MODIS land-surface temperature/emissivity products. *Remote Sensing of Environment, 112,* 59–74.

Wang W., Liang S., & Meyers, T. (2008). Validating MODIS land surface temperature products using long-term nighttime ground measurements. *Remote Sensing of Environment, 112(3),* 623-635.

Weng, Q., D. Lu, and J. Schubring, (2004). Estimation of land surface temperature-vegetation abundance relationship for urban heat island studies. Remote Sensing of Environment, 89, 467-483.

Xian, G., & Crane, M. (2005). Assessments of urban growth in the Tampa Bay watershed using remote sensing data. *Remote Sensing of Environment, 97,* 203–215.

Yang, L., Huang, C., Homer, C., Wylie, B., & Coan. M. (2002). An approach for mapping large-area impervious surfaces: Synergistic use of Landsat 7 ETM+ and high spatial resolution imagery. *Canadian Journal of Remote Sensing, 29(2),* 230-240.

Yuan, F., & Bauer, M.E. (2006). Comparison of impervious surface area and normalized difference vegetation index as indicators of surface urban heat island effects in Landsat imagery. *Remote Sensing of Environment*, *106(3)*, 375-386.

Zhang, P., M. Imhoff, R. Wolfe, and L. Bounoua. (2010). Characterizing Urban Heat Islands of Global Settlements Using MODIS and Nighttime Lights Products. Canadian Journal of Remote Sensing, Vol 36(3), pp. 185-196.

.